ISSN 1726-5479

SENSORS & TRANSDUCERS

vol. 129
6/11

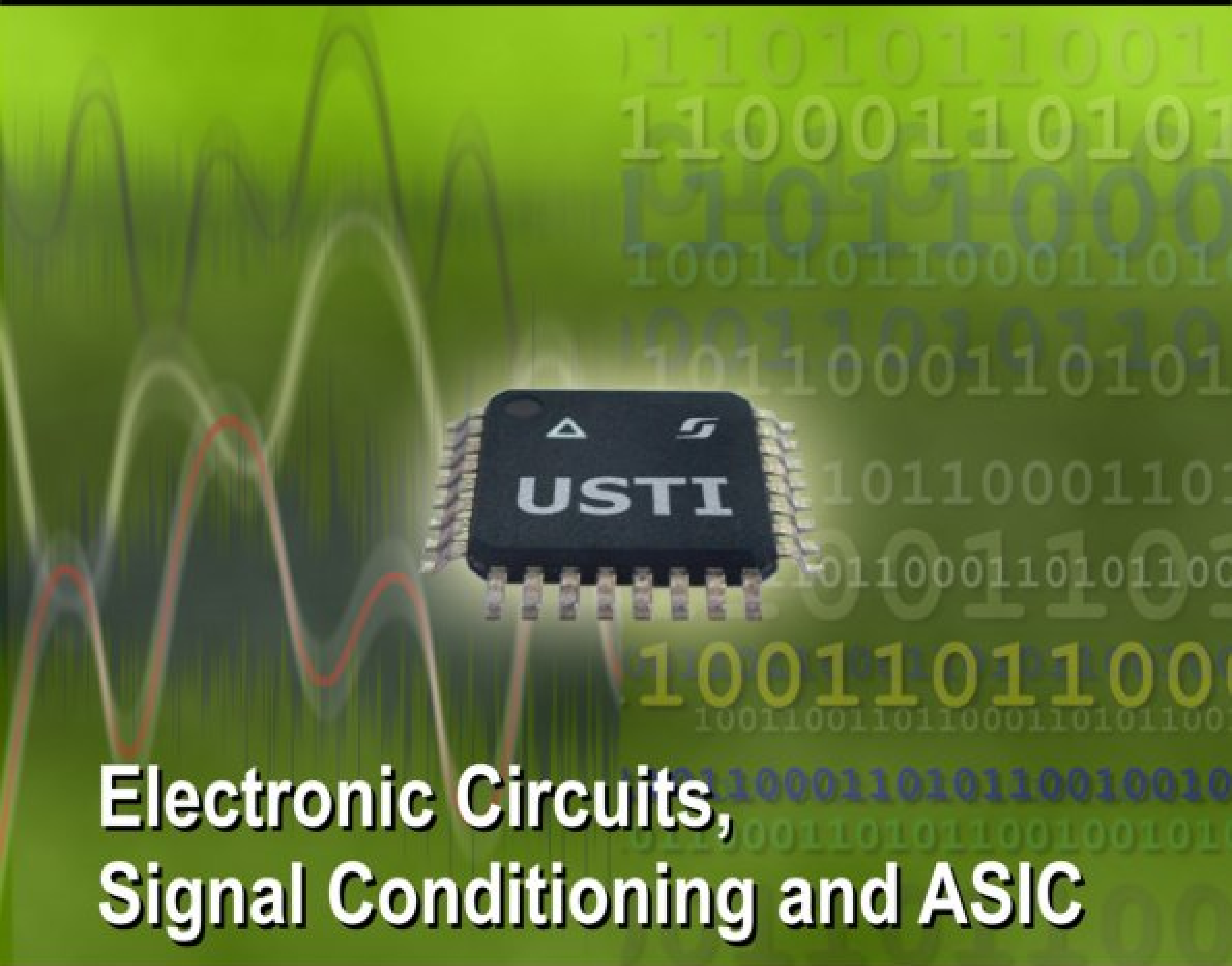

Electronic Circuits, Signal Conditioning and ASIC

International Frequency Sensor Association Publishing

IFSA

Sensors & Transducers

Volume 129, Issue 6, June 2011

www.sensorsportal.com

ISSN 1726-5479

Sensors & Transducers Journal (ISSN 1726-5479) is a peer review international journal published monthly online by International Frequency Sensor Association (IFSA).
Available in electronic and on CD.

Sensors & Transducers Journal

Contents

Volume 129
Issue 6
June 2011

www.sensorsportal.com

ISSN 1726-5479

Research Articles

Authors are encouraged to submit article in MS Word (doc) and Acrobat (pdf) formats by e-mail: editor@sensorsportal.com
Please visit journal’s webpage with preparation instructions: http://www.sensorsportal.com/HTML/DIGEST/Submition.htm

International Frequency Sensor Association (IFSA).

Sensors & Transducers Journal, Vol. 129, Issue 6, June 2011, pp. 105-121

Sensors & Transducers
ISSN 1726-5479

http://www.sensorsportal.com

Modeling of a Non-invasive Electromagnetic Sensor for the Measurement Glycaemia

A. Rouane, D. Kourtiche, [1]S. M. Alavi
Laboratory of Electronic Instrumentation of Nancy, University of Henri Poincaré-Nancy1,
BP 70239, 54506, Vandoeuvre les Nancy, France
[1]Faculty of Electrical and Computer Engineering, K.N. Toosi, University of Technology, Tehran, Iran
Tel.: +(33)383684157, fax : +(33)383684153
E-mail: amar.rouane@lien.uhp-nancy.fr

Received: 11 May 2011 /Accepted: 20 June 2011 /Published: 30 June 2011

Abstract: In this paper, we present the modeling of a non-invasive electromagnetic sensor for the measurement glycaemia. The model is based on a bio-impedance measurement. First, we optimized the dimensions of the sensor's parameters that can influence on measurement. Second, we investigated the influence of the dielectric parameters on the conductivity and its impact on the measurement of glycaemia. Results from this study demonstrate that the variation of the sensor impedance depends on the resistance and the inductance, which depend on the conductivity. The sensitivity of the output and input signal ratio strongly depends on the conductivity of the medium under investigation. Maximum conductivity at the resonance frequency was demonstrated. *Copyright © 2011 IFSA.*

Keywords: Electromagnetic sensor, Electric model sensor, Conductivity, Bio-impedance measurement, Measure, Glycaemia.

1. Introduction

Diabetes is one the most debilitating health problems in the world. The main problem of diabetes is the chronic effect of glycaemia which leads to cardiovascular diseases, diabetic neuropathy and organs failure. These complications could progress and worsen when the glycaemia is not controlled or balanced accordingly. However, frequent control and management of the glycaemia has been shown to greatly reduce the number of diabetes complications [1, 2]. Diabetic patients are required to frequently check the level of their blood glucose to avoid the secondary effects of the diabetes. Blood glucose levels are monitored daily through skin prick method, which is executed several times during the day to avoid an imbalance of blood glucose level. The prick of the skin which is painful and aversive event discourages many patients to adhere to an appropriate control of their blood glucose levels, which could lead to higher risks of diabetes complications. In order to improve the quality of life of the diabetic patients a non-invasive glucose level monitoring remains the most attractive approach for diabetic patients. A non-invasive approach will allow more frequent measurements of blood glucose without the painful sensation endured during skin prick. Several research studies have focused on developing a non-invasive method to help control glycaemia [3-6]. In the current study, we have developed an original method for a non-invasive measurement of glycaemia which is based on an electromagnetic sensor [7]. This paper focuses on the modeling of this non-invasive sensor which measures the glycaemia. This modeling is based on bio-impedance measurement [8-11]. The purpose of this study is to optimize the sensor characteristics that could influence glucose measurements. The theoretical study demonstrates that the variation of the sensor impedance, such as resistance R and inductance L, as a function of the conductivity is an important step to achieve to achieve high sensitivity.

2. Materials and Methods

The sensor consists of two induction coils coupled by a blood environment representing the solution under investigation as shown in Fig. 1. The glass tube, as an insulator, contains this solution is between the inductors and this medium. The induction wire is coiled around a 1 mm diameter glass tube. By neglecting the radius of the wire, the induction diameter is close to that of the glass tube. The length and the diameter of the inductor are 80 mm and 20 mm, respectively. The distance between the two axes of the two inductors is 40 mm. Thus, two distinct spaces are defined within inside the inductors. The first space consists of the solution under test, which can be considered as a conductor. Whereas the second space represents the hull of the glass tube which is considered as an insulator (its resistivity is $\rho \approx 2*10^{13}\,\text{ohm}*\text{m}$).

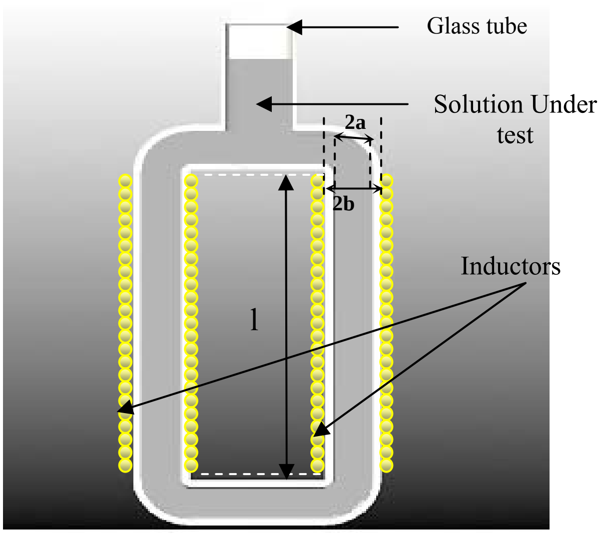

Fig. 1. Schema of the test-cell geometry.

2.1. Principle of the Sensor

We have considered a differential method for the non-invasive measurement of the glycaemia using two dimensionally identical sensors. One of the sensors allows compensation for the temperature effect. A function generator provides an input signal V_I at the resonance frequency which is applied to the first inductor of each sensor. Two outputs signal V_O and V'_O are collected on the second inductors of the two sensors. These ratios V_O/V_I, V'_O/V_I, and the difference (V_O/V_I -V'_O/V_I) are calculated using an electronic card developed in our laboratory. A detailed description of the procedure is given in [7]. In this paper, we are interested in optimizing the dimension of the sensor by calculating its impedance, and studying the influence of each parameter on the sensor.

2.2. Calculation of the Magnetic Field

Under these conditions, the magnetic field H behaves practically as an inductance in vacuum. The magnetic field H is calculated by the following equation:

$$H = \frac{nI}{\ell}, \tag{1}$$

where:
l = length of the inductor;
n = number of the spire;
I = current in the inductor;
H = magnetic field.

Assuming that $\ell \rangle\rangle b$, Fig. (1, b) represents the external diameter of the inductor, Fig. 2, and in a conductor medium, the magnetic field H should to be homogeneous at all point belonging to any straight line parallel to Z axis, Fig. 3. The magnetic field H has only one component H_Z when the field lines are parallel to Z-axis in the medium. The amplitude of the field, at any point M inside this medium depends only on the distance between this point M and the Z-axis. H(r) represents the field H inside the medium. Based on the geometry of the inductors-medium system, we choose cylindrical coordinates. The sample under test (salted water, blood, or gelatin) is a non-magnetic material suggesting that the susceptibility (χ_m) does not depend on the field H.

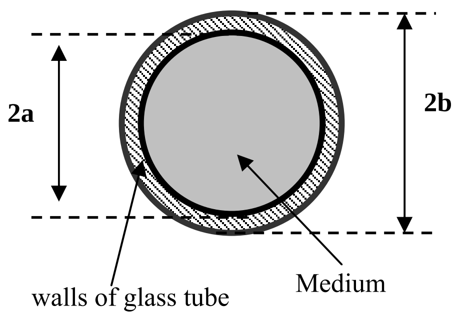

Fig. 2. Cross-section of the cell showing the medium and the walls of glass tube.

Consequently, the permeability is independent of the field H. The electromotive force E in the borders of the reel, Fig. 4, is given by:

$$E = j\,n\,\omega\,\Phi_R = V - R_0 I = (Z - R_0)I \tag{2}$$

$$= (R - R_0)I + jL\omega I \tag{3}$$

Φ_R: Resulting magnetic flux when the inductor is charged, ω: pulsation
V: Voltage at the terminals of the inductor charged by the middle.

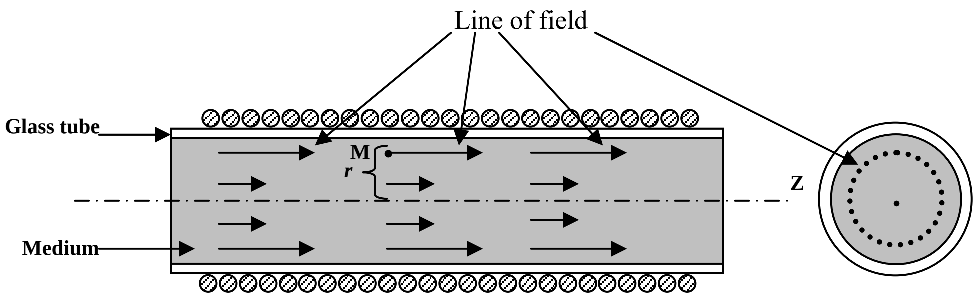

Fig. 3. Lines of magnetic field H inside the reel.

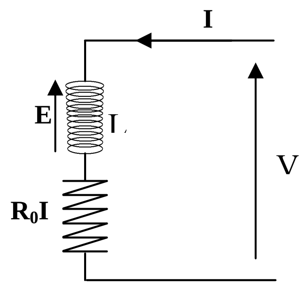

Fig. 4. Electric model of the reel.

Where

$$Z = R + jL\omega \ , \tag{4}$$

impedance of the inductor charged by the middle, and R_0 is the resistance of the reel in vacuum.

Therefore:

$$\Phi_R = -\frac{j(R - R_0)I}{n\omega} + \frac{LI}{n} \tag{5}$$

These previous relations show that we need to determine the magnetic flux, which crosses it in order to determine its impedance Z. The magnetic flux is defined by:

$$\Phi = \int \mu \, \vec{H}(\vec{r}) \, \vec{r} \, d\vec{r} \tag{6}$$

The magnetic field H(r) can be deduced from Laplace's law:

$$\Delta\vec{H} = -\overrightarrow{curl}\,\overrightarrow{curl}\,\vec{H} \tag{7}$$

Since the field H in the medium depends only on the component r, we obtain the following differential equation

$$\frac{\partial^2 H(r)}{\partial r^2} + \frac{1}{r}\frac{\partial H(r)}{\partial r} - \sigma\, j\, \mu\, \omega\, H(r) = 0 \tag{8}$$

The general solution of this equation is obtained by using Bessel's functions; details of the resolution of this equation are found in [12].

$$H(r) = nI \frac{M_0(kr)}{\ell M_0(ka)} \exp j(\theta_0(kr) - \theta_0(ka)) \tag{9}$$

M_0 and θ_0 are the amplitude and the phase of Bessel's function of first species at order 0.
n, I, ℓ, are defined above. a is the internal radius of the glass tube, Fig. 3.

The above expression of the magnetic field shows that:

- When r is close to zero (on Z-axis), then the magnetic field H becomes:

$$H(0) = nI \frac{1}{\ell M_0(ka)} \tag{10}$$

- When r is close to a, then the magnetic field H becomes:

$$H(r) = \frac{nI}{\ell} \tag{1}$$

If we attribute:

$$k^2 = \sigma \mu \omega , \tag{11}$$

then it is very useful to note that k is proportional to the permeability (μ), the pulsation (ω) and the conductivity (σ) of the medium.

2.3. Calculation of Resulting Magnetic Flux (Φ_R) and the Impedance Z

The assumption ($\ell \rangle\rangle b$) enables us to consider that the magnetic flux across all the whorls of solenoid are constant.

2.3.1. Calculation of Flux_ Φ_m

The flux Φ_m represents the magnetic flux across the medium under investigation. The magnetic flux across a surface S, of a medium exposed to a magnetic field H(r), depends only on the distance r between this point and Z-axis on the solenoid (Fig. 2). In this case:

$$\Phi_m = \int_0^a 2\pi \, \mu \, r \, H(r) dr , \tag{12}$$

where a is the radius of the medium under test.

$$\Phi_m = -j \frac{\mu \, 2\pi \, n \, I}{\ell M_0(ka)} \frac{a}{k} M_1(ka) \exp j \left[\theta_1(ka) - \theta_0(ka) - \frac{\pi}{4} \right] \tag{13}$$

M_1 and θ_1 are the amplitude and the phase of Bessel's function of first species at order 1.
M_0 and θ_0 are the amplitude and the phase of Bessel's function of first species at order 0.

2.3.2. Calculation of the Magnetic Flux Φ_v across the Walls of the Tube

The second component Φ_v denotes the magnetic flux inside the walls of the glass tube. The magnetic field in the walls of the glass tube is homogeneous, and is equal to:

$$H = \frac{nI}{\ell}. \tag{1}$$

The surface (S_1) through which the flux Φ_v flow as shown in Fig. (3), is given by:

$$S_1 = \pi \left(b^2 - a^2\right) \tag{14}$$

Thus, the flux (Φ_v) is obtained by the integral of the magnetic field $H(r) = \frac{nI}{\ell}$ (1) across all the surface (S_1) is:

$$\Phi_v = \int_0^{2\pi}\int_a^b \mu' \frac{nI}{\ell} r\, dr d\theta = \frac{\pi \mu' nI}{\ell}\left(b^2 - a^2\right), \tag{15}$$

where μ' is the permeability of the walls of the glass tube a and b are the internal and external radius, respectively, of the glass tube, Fig. 3.

2.3.3. Calculation of the Resulting Magnetic Flux Φ_R

The resulting magnetic flux (Φ_R **)** is calculated by:

$$\Phi_R = \Phi_v + \Phi_m = \frac{\pi \mu' nI}{\ell}\left(b^2 - a^2\right) - j\frac{\mu 2\pi \, n\, I}{\ell M_0(ka)} \frac{a}{k} M_1(ka) \exp j\left[\theta_1(ka) - \theta_0(ka) - \frac{\pi}{4}\right] \tag{16}$$

Thus, the identification of equations (5) and (16), allows obtaining the expressions of (R) and (L) that representing the impedance of the inductors, by the following equations:

$$R = R_0 - \frac{\mu 2\pi \, n^2 \omega}{\ell M_0(ka)} \frac{a}{k} M_1(ka) \cos\left(\theta_1(ka) - \theta_0(ka) - \frac{\pi}{4}\right) \tag{17}$$

$$L = \frac{\pi \mu' n^2}{\ell}\left(b^2 - a^2\right) - \frac{\mu 2\pi \, n^2}{\ell M_0(ka)} \frac{a}{k} M_1(ka) \sin\left(\theta_1(ka) - \theta_0(ka) - \frac{\pi}{4}\right) \tag{18}$$

The permeability of the different mediums used here, such as blood, salted water, gelatin, is practically identical to that of the glass. In this case, these variations can be considered negligible compared to other parameter as the conductivity. It follows then to consider that $\mu \approx \mu' \approx \mu_0$. Thus, the above equations can be written as follow:

$$R = R_0 - \frac{C_R\, L_0\, 2\omega}{ka} \frac{M_1(ka)}{M_0(ka)} \cos\left(\theta_1(ka) - \theta_0(ka) - \frac{\pi}{4}\right) \tag{19}$$

$$L = L_0\left[(1 - C_R) - \frac{2C_R}{ka} \frac{M_1(ka)}{M_0(ka)} \sin\left(\theta_1(ka) - \theta_0(ka) - \frac{\pi}{4}\right)\right] \tag{20}$$

where L_0 is the inductance in vacuum,

$$L_0 = \frac{\pi\, \mu_0\, b^2\, n^2}{\ell} \tag{21}$$

C_R is a factor. It corresponds to the ratio of the medium volume and the total volume inside the solenoid. It is defined by:

$$\frac{a^2}{b^2} = C_R \tag{22}$$

A simplified writing of the equations (19) and (20) gives the expressions of R and L:

$$R = R_0 + C_R\, L_0\, \omega\, f_1(ka) \tag{23}$$

$$L = L_0\left[(1 - C_R) + C_R\, f_2(ka)\right] \tag{24}$$

In our application the crucial parameter is the conductivity of our medium. Since measurements are carried out at fixed frequencies we consider all others parameters as constant, including the frequency. Taking into consideration that:

$$k = \sqrt{\sigma\, \mu\, \omega} = k'\sqrt{\sigma} \text{ with } k' = \sqrt{\omega\, \mu}\,. \tag{25}$$

The variable ka in the two above equations can be substituted by: $K\sqrt{\sigma}$, where

$$K = ak'. \tag{26}$$

We obtain the following equations as a final expression of R and L as follow:

$$R = R_0 + C_R\, L_0\, \omega\, f_1\left(K\sqrt{\sigma}\right) \tag{27}$$

$$L = L_0\left[(1 - C_R) + C_R\, f_2\left(K\sqrt{\sigma}\right)\right] \tag{28}$$

The impedance Z is calculated as follow:

$$Z = R + jL\omega = R_0 + C_R\, L_0\, \omega\, f_1\left(K\sqrt{\sigma}\right) + j\,\omega\, L_0\left[(1 - C_R) + C_R\, f_2\left(K\sqrt{\sigma}\right)\right] \tag{29}$$

In our application, the frequency, dimensions of the inductors, the permeability of the medium are constant while the conductivity is considered as the most important parameter. Consequently, the study of the impedance variation as a function of the conductivity requires the study of the two functions $f_1(\sigma)$ and $f_2(\sigma)$.

$$f_1(\sigma) = -\frac{2}{K\sqrt{\sigma}}\frac{M_1(K\sqrt{\sigma})}{M_0(K\sqrt{\sigma})}\cos\left(\theta_1(K\sqrt{\sigma}) - \theta_0(K\sqrt{\sigma}) - \frac{\pi}{4}\right) \tag{30}$$

$$f_2(\sigma) = -\frac{2}{K\sqrt{\sigma}}\frac{M_1(K\sqrt{\sigma})}{M_0(K\sqrt{\sigma})}\sin\left(\theta_1(K\sqrt{\sigma}) - \theta_0(K\sqrt{\sigma}) - \frac{\pi}{4}\right) \tag{31}$$

2.4. Study of the Impedance Variation as Function of the Conductivity

The study of impedance Z is similar to the study of the following complex function:

$$F_z = C_R \; f_1(K\sqrt{\sigma}) + j\left[(1 - C_R) + C_R\, f_2(K\sqrt{\sigma})\right] \tag{32}$$

We have developed a Matlab® program to help illustrate the variation of F_z as a function of the conductivity. Fig. (5a and b) shows the evolution of the imaginary part of F_z versus reel part of F_z at different values of C_R. The curve (5a) is plotted in the interval of $K\sqrt{\sigma}$ ranging from 0 to 50 with a step of 0.01, whereas the curve (5b) is plotted in a reduced interval ranging from 0 to 16, and with a step of 0.16. As it is demonstrated in the expression of the impedance, these curves represent the simultaneous variation of resistance R and inductance L. When the conductivity increases, we can observe two phases: an increase followed by decreases of the resistance R that corresponds to the real part of F_z and the inductance L corresponding to the imaginary part of F_z.

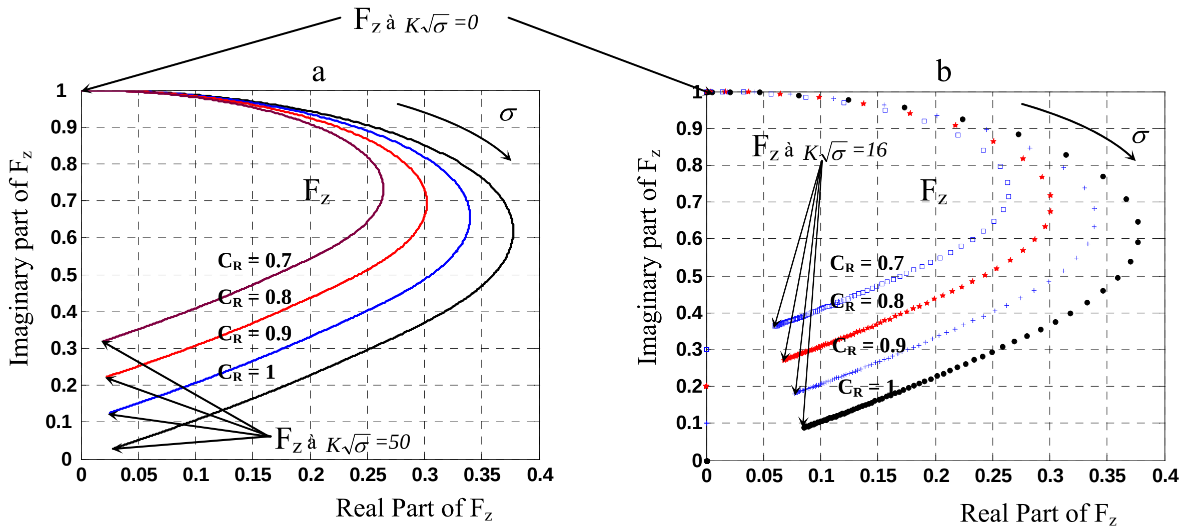

Fig. 5. Variation of F_z as a function of $K\sqrt{\sigma}$ at different value of the factor C_R.

In Fig. (5b), the step of $K\sqrt{\sigma}$ (0.16) used between two points being the same. The spaced points show that the function F_z and the impedance Z are very sensitive to the variation of conductivity in this region. When $K\sqrt{\sigma}$ increases, the points become more close indicating that the reduction in the sensitivity of F_z and therefore Z, with respect to a variation of the medium conductivity. It is also important to observe that the spacing become larger when the load factor is high.

Thus, a sensor should have a better sensitivity to the variation of medium conductivity, when the load factor is close to 1.

2.4.1. Study of the Variation of the Resistance R and the Inductance L of the Inductor as a Function of Conductivity

Basing on numerical value of the elements of each inductors of our sensor, we plotted the variations of the resistance R and inductance L as a function of the conductivity as shown in Figs. 6 and 7 respectively. The expressions (3'') and (4'') show that we need to calculate all parameters. As a first step, we need to calculate the initial values of R_0 and L_0. R_0 and L_0 do not represent the resistance and the inductance in continuous mode, but they represent the resistance and the inductance without the presence of the medium.

The capacity distributed of a solenoid results in an increase in its equivalent resistance R_0.

$$R_0 = \frac{R'_0}{\left[1-\left(\frac{f}{f_0}\right)^2\right]^2} \quad [13] \tag{34}$$

Finally we obtain (see appendix for details):

$$R_0 = 1.02 * R'_0 = 7.5 \text{ ohm.}$$

Calculation of the inductance in vacuum L_0.

The inductance in vacuum of an inductor, taking into account of its capacity distributed, is given by the equation:

$$L_0 = \frac{l_0}{1-\left(\frac{f}{f_0}\right)^2} \approx 1.015 * l_0 \approx 28.4 * 10^{-6} \text{H} \tag{35}$$

The aim of the calculation of all these parameters is to plot the curves, which give the variation of resistance R and inductance L of the sensor according to conductivity. These plots are obtained using a program developed under Matlab®.

2.4.2. Evolution of Resistance R as a Function of the Conductivity

Submitting all the parameters of the sensor by their calculated value in the equation (3'') given the expression of R, we obtain:

$$R = 7.5 + C_R \, 463 * f_1\left(K\sqrt{\sigma}\right) \tag{36}$$

Fig. 6 shows the evolution of the resistance R of our sensor as a function of the conductivity of the medium at different load factor C_R values. As indicated, for a medium with a high resistivity, the resistance R is equal to R_0 (resistance at vacuum). At high load factor (close to 1), the resistance R increases to reach approximately 182.5 Ohm. This value is about 24 times its initial value for conductivity equal approximately to 0.185 S/m. As calculated, the variation of resistance is less important if the load factor is lower.

Beyond this value of the conductivity, when σ increases to infinite value or for a medium to very high conductivity, the resistance decreases to reach its initial value 7.5 ohm, at any value of the load factor. Overall, we can say that the higher is the load factor, the more sensitivity of the sensor to the conductivity is important.

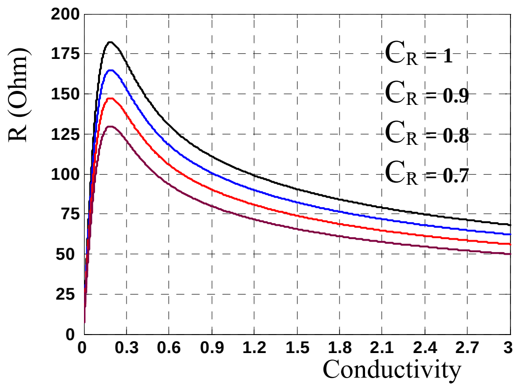

Fig. 6. Variation of the resistance as a function of the conductivity at various values of load factor.

2.4.3. Variation of Inductance L according to Conductivity

As is the case of the resistance R, submitting the elements of the sensor by their values, calculated before, we obtain the expression of L:

$$L = 28.4 * 10^{-6} \left[\left(1 - C_R\right) + C_R f_2\left(K\sqrt{\sigma}\right) \right] \quad (37)$$

Fig. 7, demonstrates the variation of the inductance (L) versus conductivity of the medium at various values of the load factor C_R . In such medium with very high resistivity, the inductance is reaching its initial value at any value of the load factor C_R .

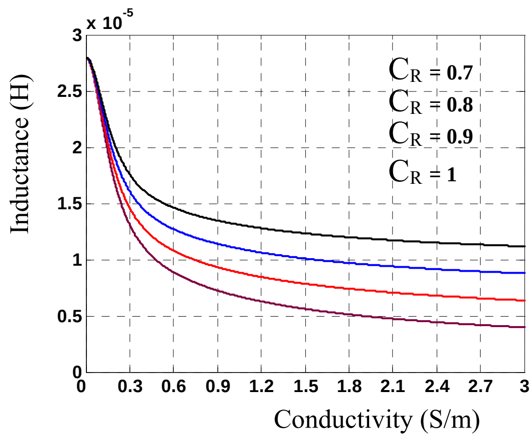

Fig. 7. Variation of the inductance (L) according to conductivity of the medium at various values of C_R .

2.5. Electric Model of the Sensor

The sensor consists of two inductors as shown in Fig. (8). A primary coil where, the alternate V_I , input signal provided by a function generator of output impedance 50 Ohm, is applied.

A second inductance through which we measured the output signal V_O. The sample under test represents the coupling that connects the two inductors. The self-capacitance of the inductor is about 1.5 pF. The self-resonance frequency of the inductor is then about 25 MHz. The resonance frequency of the sensor is between 2.5 MHz and 3MHz [12]. The schema of the electrical circuit of sensor is shown in Fig. 8.

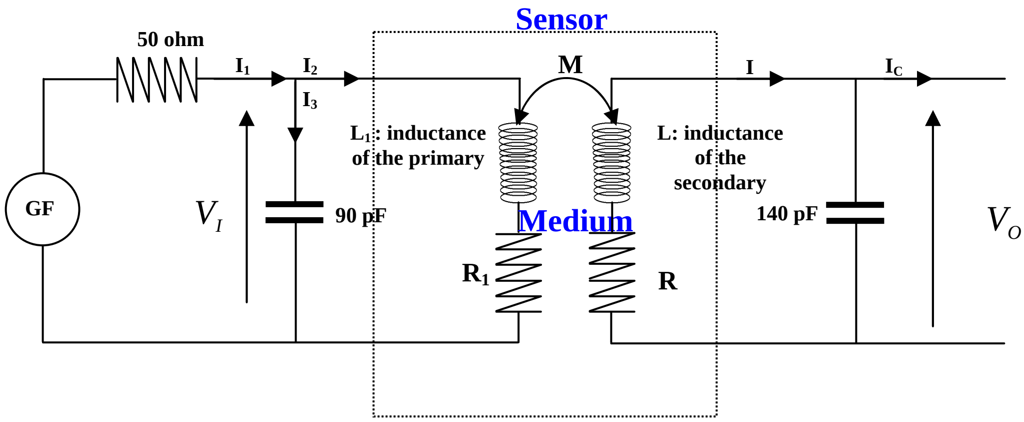

Fig. 8. Complete schema of the electrical circuit for measurement.

R, L and R_1, L_1 are the resistance and the inductance of the secondary and the primary coil of the sensor respectively. They are dependent on the medium conductivity. In this model, the variations of resistance and inductance of the two inductors are given by the following equations:

$$R = R_0 + C_R L_0 \omega f_1\left(K\sqrt{\sigma}\right) \tag{27}$$

$$R_1 = R_{01} + C_R L_{01} \omega f_1\left(K\sqrt{\sigma}\right) \tag{38}$$

$$L = L_0\left[\left(1 - C_R\right) + C_R f_2\left(K\sqrt{\sigma}\right)\right] \tag{28}$$

$$L_1 = L_{01}\left[\left(1 - C_R\right) + C_R f_2\left(K\sqrt{\sigma}\right)\right] \tag{39}$$

For flexibility, we chose to simulate the model using Matlab®. In this case, we calculate the mathematical formulas, which give the parameters to be simulated. Therefore, it is necessary to calculate the output signal V_O, the input signal V_I, the ratio V_O/V_I, and the impedance of the primary and secondary coil.

2.5.1. Calculation of the Output and Input Signal V_O, V_I, and V_O/V_I according to the Parameters of the Circuit

From the circuit shown in Fig. 8, we have the following equations:

$$Z_1 I_2 + jM\omega\sqrt{L_1 L}\ I = \frac{E\sin(\omega t)}{jR_g C_1 \omega + 1} \tag{40}$$

and

$$Z\,I \;+ jM\omega\sqrt{L_1 L}\;\; I_2 = \;0 \tag{41}$$

Where:

$$Z_1 = \left(R_1 + \frac{R_g}{1+R_1^2\,C_1^2\,\omega^2}\right) + j\left(L_1\omega - \frac{R_g^2 C_1\omega}{1+R_1^2 C_1^2\omega^2}\right) \tag{42}$$

$$Z \;=\; R + j\left(L\omega - \frac{1}{C\omega}\right) \tag{43}$$

With $I_C = 0$, we obtain the formula which gives the output signal V_O:

$$V_O \;=\; -\frac{j\;\omega\,M\sqrt{L\,L_1}\;\;E\sin(\omega t)}{\left(j\,R_g\;C_1\omega+1\right)\left(Z\,Z_1 + M^2\;LL_1\omega^2\right)} * \frac{1}{jC\omega} \tag{44}$$

The input signal V_I is expressed as:

$$V_I = \frac{\left(\left(\omega\,M\sqrt{LL_1}\right)^2 + Z*\left(R_1 + L_1\omega\right)\right)E\sin(\omega t)}{\left(j\,R_g\;C_1\omega+1\right)\left(Z\,Z_1 + M^2\;LL_1\omega^2\right)} \tag{45}$$

The ratio V_O/V_I is then expressed as:

$$V_O/V_I \;=\; -\frac{M\sqrt{L\,L_1}}{C\left(\left(\omega\,M\sqrt{LL_1}\right)^2 + Z*\left(R_1 + L_1\omega\right)\right)} \tag{46}$$

with M: the mutual inductance; other symbols have been identified.

The impedance Z will be substituted by the values of R, L, R_1, L_1, given previously in its expression, and the functions f_1, f_2 take the same expression respectively. As it can be seen, the ratio V_O/V_I is independent of the amplitude of the input signal. The study and the simulation of these equations were carried out using a program developed under Matlab® software. The curves are plotted as a function of the frequency and of the conductivity σ. The amplitude of the input signal used in these simulations is of 12 Volts.

3. Results and Discussion

3.1. Simulation of the Impedance Z Variation

Fig. 9 shows the simultaneous variation of the impedance Z of the secondary coil as a function of frequency and the conductivity of the medium, especially, at its minimum point.

At a frequency equal to 2.325 MHz and for conductivity practically null, the curve shows well that impedance Z reached its minimal value (denoted point A). When conductivity increases, this minimum point shifts towards the left at a higher frequency as the arrow indicates it. In addition, when the conductivity of the medium increases, the impedance Z of the minimum (point A) of the curve also increases until reaching a value equal to 48.7 ohm for a conductivity which closes to approximately

0.24. When the conductivity is higher than 0.24 the impedance Z decreases. The impedance Z shows sensitivity to the variation of conductivity

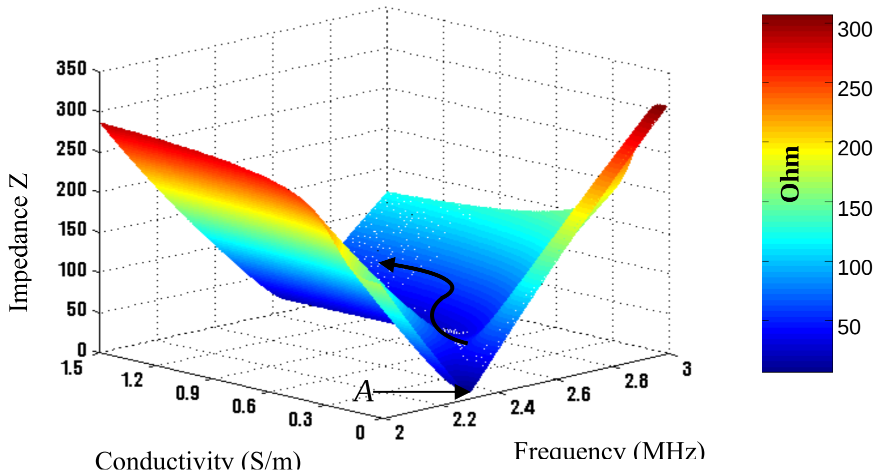

Fig. 9. Simultaneous variation of the impedance Z of the secondary coil in the frequency range (2-3MHz) and the conductivity of the medium.

3.2. Simulation of the Variation of the Amplitude of the Ratio V_O/V_I

Fig. 10 illustrates the 3D representation of the amplitude variation of the ratio of the output signal V_O and the input signal as a function of frequency and of conductivity of the medium. The curve shows that the resonance frequency shifts towards the left when conductivity increases. That is due to the decrease in inductance when the conductivity increases, as it was illustrated on Fig. (7). We can also observe that the amplitude of the ratio V_O/V_I shows two phases: The amplitude quickly decreases to increase afterward when the conductivity continues to increase more.

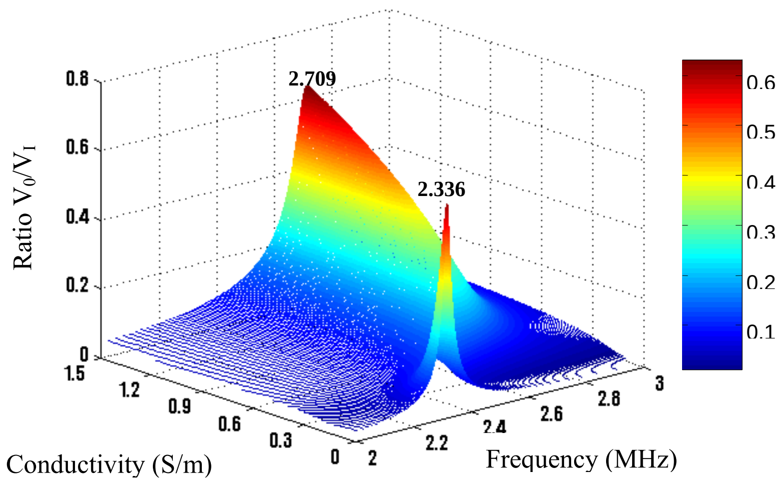

Fig. 10. Evolution of the ratio of the amplitude in the frequency (2-3MHz) and according of the conductivity of the medium.

This variation of amplitude is due basically to the direct variation of the function $F_Z(K\sqrt{\sigma})$, as it was shown before on Fig. (5). At the resonance frequency (2.324 MHz) the ratio reaches 0.619 for a medium, where the conductivity is practically zero. The amplitude decreases quickly to reach a value of 0.135 during the transition from an insulating medium to a slightly conducting medium. In contrast, the amplitude of the ratio increases to reach a value of 0.638 at a frequency of 2.716 MHz. The curve shows a shift of the resonance frequency when the conductivity increases.

The sensitivity of the ratio V_O/V_I to the variation of the conductivity of the medium is higher at the resonance frequency. This sensitivity to the variation of conductivity is very important than that of the output signal V_O (this study will be presented later). For example, at the resonance frequency, the amplitude ratio between a medium of conductivity 1.5 S/m and another of 0.75 S/m, the ratio of the output signals V_O (1.5 S/m)/ V_O (0.75 S/m) gives 1.56, whereas the ratio V_O/V_I (1.5 S/m)/ V_O/V_I (0.75 S/m) gives 1.64. In other words, the change of conductivity from 0.75 to 1.5 the output voltage increases by 56 %, while the ratio V_O/V_I increases by 64%.

The shift of the resonance frequency as shown in these curves is mainly due to the variation of the inductance (L) of the inductors as it was shown on Fig. 7. While the variations of amplitude at the same time is due to the variation of the resistance R of the inductors and to the variation of its inductance, as it was illustrated on Fig. 6 and Fig. 7 respectively, or quite simply with the variation of function $F_Z(K\sqrt{\sigma})$ as it was shown on Fig. 5.

4. Conclusion

In this work, we studied a model of the non-invasive sensor for the measurement of glycaemia. This model is based on the calculation of the expression of the flux through each inductor of the sensor. Contrary to an insulating medium, we demonstrated that the flux is a complex quantity in a conducting medium, The inductors are considered as a long solenoid, which is the case of the inductors that constitute our sensor. In order to analyze the complex equations included in our model, we have developed a Matlab® program. This program also allows studying the influence of the various parameters such as radius of inductors, frequency, factor of filling. Using a simple modification to the program, we have examined whether an increase in the radius of the inductance could improve the sensitivity of the sensor. Results from different curves are plotted indicating the variation of the various signals according to the conductivity of the medium under test. All magnitudes of V_O, V_I and V_O/V_I showed an important sensitivity to the variation of conductivity. The ratio V_O/V_I combines the sensitivity of V_O and of V_I. These simulation data requires further examination under experimental measurements [14, 15].

Appendix

The capacity distributed of a solenoid results in an increase in its equivalent resistance R_0.

$$R_0 = \frac{R'_0}{\left[1-\left(\frac{f}{f_0}\right)^2\right]^2} \text{ [13]} \tag{A1}$$

It is necessary to calculate the resistance R'_0 first of all, which represents the resistance of the inductor without its capacitance, and its-self frequency f_0 of this inductor. We use the relation [13]:

$$\frac{R'_0}{r_0} = \frac{r}{2\delta} K(r/s, \ell/D) \tag{A2}$$

K(r/s, ℓ/D) represents a correction function due to the proximity effect on the resistance of the coil at high frequency.

Where:

r_0 is the resistance in continuous mode and it is given by:

$$r_0 = \frac{\rho l}{s} \approx 0.33 \text{ ohm.} \tag{A3}$$

r represents the radius of the wire, which is equal to 0.5 mm.

ℓ, s, ρ, D are the length, the section, the resistivity and the diameter respectively of the coil.

The penetration depth is calculated by the relation:

$$\delta = \frac{\sqrt{2}}{\sqrt{\mu_{cu}\sigma_{cu}\,\omega}} = 4*10^{-5} \text{ m} \tag{A4}$$

This value is calculated at fixed frequency (F= 2.6 MHz). μ_{cu}, σ_{cu} are the permeability and the conductivity of the copper wire, respectively. The calculation of the function (Medhurst's theory) K($r/s, \ell/D$) [13] equals to 3.5, when the length of the inductor is 80 mm, its diameter is 20 mm and that winding is tight. Then, we obtain the value of $R'_0 = 7.3$ Ohm.

Calculation of f_0

f_0 is defined by:

$$f_0 = \frac{1}{2\pi\sqrt{Cl_0}} \tag{A5}$$

where C is the distributed capacity C of the inductor, l_0 is the inductance of the inductors without its self-capacitance C.

a. Calculation of C

For a solenoid with only one layer, the formula [13]

$$C = AD/10, \tag{A6}$$

is an approximation, which is often used in practice to evaluate this capacity. D is the diameter of the solenoid, and A is a coefficient that depends on the ratio of the length ℓ of the solenoid to its diameter. The distributed capacity of this inductance is then: $C \approx 1.5\,\text{pf}$.

b. Calculation of l_0

This result gives the inductance in vacuum of a solenoid without taking into account the effect of the distributed capacity C:

$$l_0 = K_c\, l'_0 \tag{A7}$$

With K_c is the Nagaoka's corrective factor [13] and l'_0 is the inductance of the solenoid in vacuum. Considering it very long, and by neglecting the edge effect, l_0 is given by:

$$l'_0 = N^2 \mu_0 \frac{D^2}{\ell}\frac{\pi}{4} \approx 31.5 * 10^{-6}\,H, \tag{A8}$$

where N is the number of whorls of the reel, μ_0 the permeability in vacuum, D and ℓ are the diameter and the length of the inductor respectively. The length of our solenoid is four times larger than its diameter. Using Nagaoka's corrective factor of ($K_c \approx 0.9$) then we obtained: $l_0 \approx 28 * 10^{-6}\,H$. The value of Nagaoka's corrective factor K_c is obtained from the curve, Fig. A1, who traces this factor K_c according to the ratio D/ℓ [13].

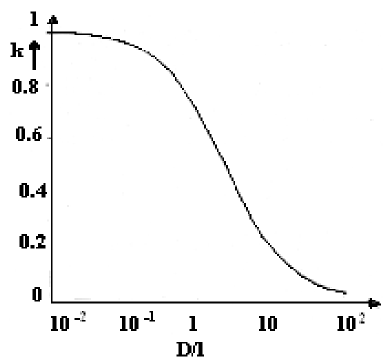

Fig. A1. The value of Nagaoka's corrective factor K_c for various values of the ratio D/l.

Thus that its-self resonance frequency of the inductor is: $f_0 = \frac{1}{2\pi\sqrt{Cl_0}} \approx 2.5 * 10^7$ Hz. Since the maximum frequency of working band is 3 MHz, this gives a maximum ratio of:
$\frac{f}{f_0} \approx 0.12$. Finally we obtain: $R_0 = 1.02 * R'_0 = 7.5$ ohm.

References

[1]. The Diabetes Control and Complications Trial Research Group, The effect of intensive treatment of diabetes on the development and progression of long-term complications in insulin-dependent diabetes mellitus, *N Engl J Med*, 329, 1993, pp. 977-986.

[2]. Updike, S. J., Shults, M. C., Gilligan, B. J., Rhodes, R. K., A subcutaneous glucose sensor with improved longevity, dynamic range, and stability of calibration, *Diabetes Care,* 23, 2000, pp. 208-214.

[3]. Ok Kyung C., Yoon Ok K., Hiroshi M. and Katsuhiko K., Non-invasive Measurement of Glucose by Metabolic Heat Conformation Method, *Clinical Chemistry,* 50, 10, 2004, pp. 1894–1898.

[4]. Omar S. Khalil, Non-Invasive Glucose Measurement Technologies: An Update from 1999 to the Dawn of the New Millennium, *Diabetes Technology & Therapeutics,* Vol. 6, No. 5, Oct 2004, pp. 660 -697.

[5]. David C. K., Continuous Glucose Monitoring Technology Delivers Detailed Diabetes Data, Point of Care, *The Journal of Near-Patient Testing & Technology*, Vol. 5, No. 3, 2006, pp. 105.

[6]. Yamakoshi K., Yamakoshi Y., Pulse glucometry: a new approach for noninvasive blood glucose measurement using instantaneous differential near-infrared spectrophotometry, *Journal of Biomedical Optics.,* Vol. 11, No. 5, 2006, pp. 054028.

[7]. Gourzi, M., Rouane, A., Guelaz, R., Nadi, M., Jaspard, F., Study of a new electromagnetic sensor for glycaemia measurement: in-vitro results on blood pig, *Journal of Medical Engineering & Technology,* Vol. 627, 2003, pp. 276 – 281.

[8]. Critchley, L. A., Calcroft, R. M., Tan, P. Y., Kew, J., and Critchley, J. A., The effect of lung injury and excessive lung fluid, on impedance cardiac output measurements, in the critically ill, *Intensive Care Med,* 26, 2000, pp. 679-685.

[9]. Young, J. D., and Mc. Quillan, P., Comparison of thoracic electrical bio impedance and thermo dilution for the measurement of cardiac index in patients with severe sepsis, *Br J Anaesth,* 70, 1993, pp. 58-62.

[10]. Hirschl, M. M., Kittler, H., Woisetschlager, C., Siostrzonek, P., Staudinger, T., Kofler, J., Oschatz, E., Bur, A., Gwechenberger, M., and Laggner, A. N., Simultaneous comparison of thoracic bio-impedance and arterial pulse waveform-derived cardiac output with thermo-dilution measurement, *Crit Care Med,* 28, 2000, pp. 1798-1802.

[11]. Summers, R. L., Kolb, J. C., Woodward, L. H., and Galli, R. L., Diagnostic uses for thoracic electrical bio-impedance in the emergency department: clinical case series, *Eur J Emerg Med,* 6, 1999, pp. 193-199.

[12]. Gourzi M., Modélisation théorique et expérimentale d'un système de mesure électromagnétique non invasif : Application à la mesure de la glycémie, *Thesis of Henri Poincaré's University,* Nancy, France, 2004.

[13]. Grivet P., Legros Roger, Physique des circuits, Ed. Masson&Cie, 1960, pp. 291-324.

[14]. Gourzi M, Rouane A., Guelaz, R., M. S. Alavi, McHugh M. B., Nadi M. and Roth P., Non-invasive glycaemia blood measurement by electromagnetic sensor: Study in static and dynamic blood circulation, *Journal of Medical Engineering & Technology,* Vol. 29, 1, 2005, pp. 22–26.

[15]. Gourzi, M., Rouane, A., Guelaz, R., Nadi, M., New biosensor for non-invasive glucose concentration measurement, *The 2nd IEEE International Conference on Sensor,* Toronto, Canada, 4, 2003, pp. 480-482.

Guide for Contributors

Aims and Scope

Sensors & Transducers Journal (ISSN 1726-5479) provides an advanced forum for the science and technology of physical, chemical sensors and biosensors. It publishes state-of-the-art reviews, regular research and application specific papers, short notes, letters to Editor and sensors related books reviews as well as academic, practical and commercial information of interest to its readership. Because of it is a peer reviewed international journal, papers rapidly published in *Sensors & Transducers Journal* will receive a very high publicity. The journal is published monthly as twelve issues per year by International Frequency Sensor Association (IFSA). In additional, some special sponsored and conference issues published annually. *Sensors & Transducers Journal* is indexed and abstracted very quickly by Chemical Abstracts, IndexCopernicus Journals Master List, Open J-Gate, Google Scholar, etc. Since 2011 the journal is covered and indexed (including a Scopus, Embase, Engineering Village and Reaxys) in Elsevier products.

Topics Covered

Contributions are invited on all aspects of research, development and application of the science and technology of sensors, transducers and sensor instrumentations. Topics include, but are not restricted to:

- Physical, chemical and biosensors;
- Digital, frequency, period, duty-cycle, time interval, PWM, pulse number output sensors and transducers;
- Theory, principles, effects, design, standardization and modeling;
- Smart sensors and systems;
- Sensor instrumentation;
- Virtual instruments;
- Sensors interfaces, buses and networks;
- Signal processing;
- Frequency (period, duty-cycle)-to-digital converters, ADC;
- Technologies and materials;
- Nanosensors;
- Microsystems;
- Applications.

Submission of papers

Articles should be written in English. Authors are invited to submit by e-mail editor@sensorsportal.com 8-14 pages article (including abstract, illustrations (color or grayscale), photos and references) in both: MS Word (doc) and Acrobat (pdf) formats. Detailed preparation instructions, paper example and template of manuscript are available from the journal's webpage: http://www.sensorsportal.com/HTML/DIGEST/Submition.htm Authors must follow the instructions strictly when submitting their manuscripts.

Advertising Information

Advertising orders and enquires may be sent to sales@sensorsportal.com Please download also our media kit: http://www.sensorsportal.com/DOWNLOADS/Media_Kit_2011.pdf